Tunable entanglement resource in elastic electron-exchange collisions out of chaotic spin systems

B. Lohmann,[1,*] K. Blum,[1] and B. Langer[2]

[1]*Institut für Theoretische Physik, Westfälische Wilhelms-Universität Münster, Wilhelm-Klemm-Strasse 9, 48149 Münster, Germany*

[2]*Physikalische Chemie, Freie Universität Berlin, Taku-Strasse 3, 14195 Berlin, Germany*

(Received 5 July 2016; published 29 September 2016)

Elastic collisions between initially unpolarized electrons and hydrogenlike atoms are discussed aiming to analyze the entanglement properties of the correlated final spin system. Explicit spin-dependent interactions are neglected and electron exchange only is taken into account. We show the final spin system to be completely characterized by a single spin correlation parameter depending on scattering angle and energy. Its numerical value identifies the final spins of the collision partners to be either in the separable, entangled, or Bell correlated regions. The symmetry of the scattering process allows for the construction of explicit examples applying methods of classical communication and local operations for illustrating the concepts of nonlocality versus separability. It is shown that strong correlations can be produced violating Bell's inequalities significantly. Furthermore, the degree of entanglement can be continuously varied simply by changing either the scattering angle and/or energy. This allows for the generation of tunable spin pairs with any desired degree of entanglement. It is suggested to use such nonlocally entangled spin pairs as a resource for further experiments, for example in quantum information processes.

DOI: 10.1103/PhysRevA.94.032331

I. INTRODUCTION

Quantum entanglement and nonlocality are continuously at the center of intense research activities [1–3]. This involves the foundations of quantum theory with regard to the Einstein-Podolsky-Rosen criticism [4] as well as Bell's theorem [5], both intended trying to preserve the Newtonian local realistic picture. Over the decades, violation of Bell's inequalities [5,6] have been observed experimentally in a variety of physical systems, e.g., see [7]. Only recently, considerable progress has been achieved, almost simultaneously, by Hensen *et al.* [8], Giustina *et al.* [9], and Shalm *et al.* [10] who have been able to reject the hypothesis of local realism with remarkable statistical significance, removing essentially the last serious doubts on the existence of nonlocal interactions in nature.

A second line of research started with the advent of quantum information theory, recognizing entanglement, established by Schrödinger [11] as *Verschränkung*, as a resource for tasks like quantum cryptography [12,13], quantum teleportation [14], or quantum computation [15,16]. This led to a rapidly growing interest in entanglement theory and quantum nonlocality, both dealing with different aspects of one of the most intriguing peculiarities of nature, and many experiments today aim at the generation of entanglement; e.g., see [1–3].

Most research so far utilized variations of entangled photons in the experimental setups in order to reject local realism. One aim of the present paper is to supplement these results by following different and new paths, opened up in our previous research [17], by studying the spin-spin correlations created in elastic electron-atom collisions. It will be shown that strong correlations can be obtained, violating Bell's inequalities even maximally in some cases. This is direct proof of the inherent nonlocality of the spin-spin system under discussion and is in support of the results given in [8–10]. Our second aim is to show that these nonlocally entangled spin pairs of the collision partners might be used as a resource in sophisticated experiments relying on a high degree of entanglement, for example in quantum computation. As an interesting feature, the degree of entanglement can be continuously tuned in such experiments, simply by changing the relevant scattering angle or energy.

Spin-dependent collisions between electrons and atoms have been studied for many years with increasing precision and efficiency, aiming to obtain information on the scattering dynamics [18,19]. More recently, entanglement properties in photon-induced ionization have been reported [20]. In the present paper we will analyze collisions between initially unpolarized electrons and unpolarized hydrogenlike atoms (H, Li, Na), both having electronic spin-1/2, and study the interrelation between scattering dynamics and the creation of nonlocal correlations, starting from a maximally chaotic initial spin state. We assume all explicit spin-dependent forces to be neglected and electron exchange to be taken into account, only. It will be demonstrated that the final state spin density matrix is completely expressed in terms of a single dynamical parameter characterizing the spin-spin correlations, while its numerical value determines whether the final spin system remains separable, or becomes entangled, or even Bell correlated, i.e., it violates any of the Bell inequalities [5,6]. Such studies unveil, as fundamental aspects, the completely different nature of spin correlations for separable and entangled states. As a consequence, the presence of entangled spin pairs in the final beams can be verified experimentally on the basis of one local measurement. By adapting existing experimental and numerical results we will obtain data for the correlation parameter and are then able to analyze the entanglement properties of the final collision system.

The present paper is organized as follows. A general expression for the spin density matrix of the final scattering system will be derived in Sec. II, while in Sec. III it will be shown that, as a main result, the final spin system is completely characterized in terms of a single spin correlation parameter, which yields, so to speak, the link between collision dynamics

*lohmanb@uni-muenster.de

and quantum mechanical entanglement. It is shown that spin correlation data can be obtained from measurements of the spin asymmetry, thereby avoiding the performance of a difficult spin-selective coincidence experiment (see the Appendix). In Sec. IV specific criteria will be applied in order to decide about the separability or nonseparability of the final state density matrix. It is demonstrated that the spin correlation parameter contains the full information on the entanglement properties and governs separability, entanglement, or Bell correlation of the final state spin system. The following three sections are devoted to a discussion of these different properties. The abstract concept and physical importance of separability will be illustrated in Sec. V. It will be shown that, in the separable region, the spin-spin correlations are of classical nature, and the spin system is indistinguishable from a system prepared locally in a classical way. Explicit examples for correlated and anticorrelated spins will illustrate these concepts which will also be useful for the discussion later on. For predominantly anticorrelated spins the final state spin density matrix can be written in form of a *Werner state* [21]. These states have high conceptual value in discussing fundamentals of quantum mechanics. In the entangled region, considered in Sec. VI, we will introduce the concept of negativity in order to quantify the amount of entanglement generated during the scattering process. In Sec. VII we will discuss the relation between entanglement and Bell correlations. Conditions are derived required for the production of inherently nonlocal spin pairs. Section VIII is an essential part of the paper. The theory, developed in the previous sections, will be applied for analyzing published experimental and numerical spin asymmetry data, out of which the corresponding values for the spin correlation parameter can easily be obtained. A detailed analysis will allow for a deep insight into the entanglement properties of the final state spin pairs. The results will reveal that surprisingly strong spin correlations can be created during the collision which in some cases violate Bell's inequalities even maximally, indicating large nonlocal effects. Furthermore, the dependence of the spin correlation parameter on scattering angle and energy allows for generating spin pairs with any desired degree of entanglement, simply by changing the experimental conditions. Hence, the scattered particles can be used, for example, as a resource of strongly correlated spin pairs for further experiments. All in all, the collision system under discussion can be utilized as a useful means for studying and applying nonlocal effects in quantum theory. Possible applications in quantum information and quantum computation will be pointed out. In Sec. IX we will summarize our main results. A possible spin resolved experimental coincidence analysis of the spin-spin correlations is outlined in the Appendix.

II. DENSITY MATRIX OF THE FINAL STATE

Our main goal in Secs. II and III is the derivation of expressions (14) and (16), which contain the key results for all following discussions, and to introduce relation (21) which is essential for the discussion of existing experimental and numerical data in Sec. VIII.

In order to describe the elastic scattering within the combined electron-atom system, while neglecting spin-orbit interaction, we express the initial unpolarized state by the density matrix

$$\rho_{\rm in} = \frac{1}{4}\sum_{m_1 m_2} |m_1 m_2\rangle\langle m_1 m_2|, \tag{1}$$

being an incoherent superposition of the equally distributed spins, where m_1 and m_2 denote the spin components of the first (electrons) and second particle (atoms), respectively. The density matrix, characterizing the final state after the scattering, is given by the relation

$$\rho = T\rho_{\rm in}T^{+}, \tag{2}$$

where T is the transition operator. Taking matrix elements (M_i and m_i denote spin components in the final and initial states, respectively) we obtain

$$\langle M_1' M_2'|\rho|M_1 M_2\rangle = \frac{1}{4}\sum_{m_1 m_2}\langle M_1' M_2'|T|m_1 m_2\rangle \times \langle m_1 m_2|T^{+}|M_1 M_2\rangle. \tag{3}$$

Here scattering angle and energy are assumed to be fixed and their dependence on the scattering amplitudes is suppressed. In the T-matrix elements we couple to the total spin S and its component M_s with the help of Clebsch-Gordan coefficients

$$\langle M_1 M_2|T|m_1 m_2\rangle = \sum_{SM_s}(1/2M_1,1/2M_2|SM_s) \times(1/2m_1,1/2m_2|SM_s)\langle SM_s|T|SM_s\rangle, \tag{4}$$

where conservation of the total spin and its component has been applied. Using the fact that the T matrix is independent of M_s, we introduce

$$\langle SM_s|T|SM_s\rangle = f^{(S)}, \tag{5}$$

where $f^{(S)}$ denote the triplet ($S=1$) and singlet ($S=0$) scattering amplitudes, respectively.

Substituting (4) and (5) into (3) and using the orthogonality of the Clebsch-Gordan coefficients finally yields

$$\langle M_1' M_2'|\rho|M_1 M_2\rangle = \frac{1}{4}\sum_{SM_s}(1/2M_1',1/2M_2'|SM_s)(1/2M_1,1/2M_2|SM_s)|f^{(S)}|^2. \tag{6}$$

For the following it is useful to write the density matrix ρ in explicit matrix form. Inserting numerical values for the Clebsch-Gordan coefficients into (6), we obtain as a preliminary result the 4×4 matrix

$$\rho = \frac{1}{8\sigma}\begin{pmatrix} 2|f^{(1)}|^2 & 0 & 0 & 0 \\ 0 & |f^{(1)}|^2 + |f^{(0)}|^2 & |f^{(1)}|^2 - |f^{(0)}|^2 & 0 \\ 0 & |f^{(1)}|^2 - |f^{(0)}|^2 & |f^{(1)}|^2 + |f^{(0)}|^2 & 0 \\ 0 & 0 & 0 & 2|f^{(1)}|^2 \end{pmatrix}. \tag{7}$$

Here ρ is normalized by the differential cross section

$$\sigma = \tfrac{1}{4}(3|f^{(1)}|^2 + |f^{(0)}|^2), \tag{8}$$

and $\mathrm{tr}\ \rho = 1$.

III. SPIN CORRELATIONS

The spin density matrix (7) can be completely characterized in terms of the two individually measured polarization vectors $\boldsymbol{P}^{(1)}$ and $\boldsymbol{P}^{(2)}$, referring to particles 1 and 2,

$$P_i^{(1)} = \mathrm{tr}\,\rho(\sigma_i \times \mathbb{1}) \quad \text{and} \quad P_i^{(2)} = \mathrm{tr}\,\rho(\mathbb{1} \times \sigma_i), \tag{9}$$

where $i = x,y,z,\mathbb{1}$ is the two-dimensional unit matrix, and $\times$ denotes the direct product, and the nine direct product components $P_i^{(1)} \times P_j^{(2)}$ of the spin-spin correlation tensor $(i,j = x,y,z)$, defined by the expression [22]

$$P_i^{(1)} \times P_j^{(2)} = \mathrm{tr}\,\rho(\sigma_i \times \sigma_j), \tag{10}$$

where σ_i $(i = x,y,z)$ abbreviate the Pauli matrices:

$$\sigma_x = \begin{pmatrix} 0 & 1 \\ 1 & 0 \end{pmatrix}, \quad \sigma_y = \begin{pmatrix} 0 & -i \\ i & 0 \end{pmatrix}, \quad \text{and} \quad \sigma_z = \begin{pmatrix} 1 & 0 \\ 0 & -1 \end{pmatrix}. \tag{11}$$

If both subsystems are completely uncorrelated, i.e., if $\rho = \rho^{(1)} \times \rho^{(2)}$, then (10) reduces to the simple product of the individual polarization vectors

$$P_i^{(1)} \times P_j^{(2)} = P_i^{(1)} \cdot P_j^{(2)}. \tag{12}$$

The correlation parameters refer to experiments where both scattered particles are measured in coincidence by two observers. For example, $P_z^{(1)} \times P_z^{(2)}$ gives the outcome of an experiment where both analyzer-detector sets are oriented along the z direction, which yields [22]

$$P_z^{(1)} \times P_z^{(2)} = \frac{1}{N}\big(N(z)_{\uparrow\uparrow} + N(z)_{\downarrow\downarrow} - N(z)_{\uparrow\downarrow} - N(z)_{\downarrow\uparrow}\big), \tag{13}$$

where, e.g., $N(z)_{\uparrow\uparrow}$ denotes the number of measurements finding both particles with spin up with respect to the z axis. The spin-selective detectors in such an experiment can be realized by a Stern-Gerlach analyzer and Mott polarimeter techniques for the atomic and electronic spins, respectively [23]. A possible scheme of an e-H spin correlation experiment is depicted in Fig. 8 of the Appendix for illustrative purposes.

The simple structure of the density matrix (7) allows for quickly calculating the relevant parameters. The individual polarization vectors of the two subsystems cancel, and the only nonvanishing spin correlation parameters are

$$P = P_i^{(1)} \times P_i^{(2)} = \frac{|f^{(1)}|^2 - |f^{(0)}|^2}{3|f^{(1)}|^2 + |f^{(0)}|^2}, \quad i = x,y,z, \tag{14}$$

where we introduced the parameter $P = P(\theta,E)$ which is a function of scattering angle and energy.

Equation (14) can be generalized applying the tensorial properties of $P_i^{(1)} \times P_i^{(2)}$. Let $\sigma_a = \boldsymbol{\sigma} \cdot \boldsymbol{a}$ denote the component of the Pauli operator $\boldsymbol{\sigma}$ in the direction of the unit vector $\boldsymbol{a}$, and $\sigma_b = \boldsymbol{\sigma} \cdot \boldsymbol{b}$ denote the component in direction $\boldsymbol{b}$. If the spin of the first particle is measured along direction $\boldsymbol{a}$, and the spin of the second particle along $\boldsymbol{b}$, the resulting correlations are given by the expression

$$P_a^{(1)} \times P_b^{(2)} = P\cos\beta, \tag{15}$$

where β is the angle between $\boldsymbol{a}$ and $\boldsymbol{b}$ [22]. This, together with (14), exhibits the rotational symmetry of the spin-spin system. Using (8) and (14) we can express the spin density matrix (7) in terms of the spin correlation parameter. We obtain

$$\rho = \frac{1}{4}\begin{pmatrix} 1+P & 0 & 0 & 0 \\ 0 & 1-P & 2P & 0 \\ 0 & 2P & 1-P & 0 \\ 0 & 0 & 0 & 1+P \end{pmatrix}. \tag{16}$$

Equation (16) shows that the spin system under discussion is completely characterized by the single parameter P. In contrast, for a most general scattering experiment, e.g., including spin-orbit interaction and more general initial conditions, the density matrix can depend on up to 15 independent parameters. In general, the values of the correlation parameter are restricted to the interval $[-1,1]$. From (14) we get the further restriction

$$-1 \leqslant P \leqslant \frac{1}{3}. \tag{17}$$

The spin density matrix (16) provides the key equation. From its structure, (16) represents a so-called X matrix, with only diagonal and antidiagonal elements, which has been used in the analyses of two-qubit quantum systems [24,25]. Its simple structure will allow for a transparent discussion of all entanglement properties of the final spin system. Note that the density matrix (16) admits the Bloch representation

$$\rho = \frac{1}{4}\left(\mathbb{1} + P\sum_i \sigma_i \times \sigma_i\right), \quad i = x,y,z, \tag{18}$$

where $\mathbb{1}$ denotes the four-dimensional unit matrix.

A spin selective coincidence experiment as described above is not easy to perform. Therefore, it is important to note that the

correlation parameter (14) can also be obtained from the results of a different type of experiment, where many experimental and numerical results are already available. Consider the case where electrons and atoms, both, are initially polarized. Then, the spin asymmetry $A_{\rm ex}$ can be measured which is defined as

$$A_{\rm ex} = \frac{\sigma_{\uparrow\downarrow} - \sigma_{\uparrow\uparrow}}{\sigma_{\uparrow\downarrow} + \sigma_{\uparrow\uparrow}}, \tag{19}$$

where $\sigma_{\uparrow\downarrow}$ and $\sigma_{\uparrow\uparrow}$ denote differential cross sections for incident antiparallel and parallel spins, respectively. Expressing $A_{\rm ex}$ in terms of the scattering amplitudes $f^{(0)}$ and $f^{(1)}$, we obtain [26]

$$A_{\rm ex} = \frac{|f^{(0)}|^2 - |f^{(1)}|^2}{3|f^{(1)}|^2 + |f^{(0)}|^2}. \tag{20}$$

A comparison with (14) yields the simple relation

$$P(\theta, E) = -A_{\rm ex}(\theta, E). \tag{21}$$

Using published data for the spin asymmetry $A_{\rm ex}$, then (21) allows us to immediately obtain the spin correlation parameter P for our considered experimental setup with initially unpolarized particles (see the discussion in Sec. VIII later on).

IV. ENTANGLEMENT VERSUS SEPARABILITY: PERES-HORODECKI CRITERION

We now discuss under which conditions the mixed spin state (16) is separable or entangled, or a combination of both. Generally, a density matrix of a bipartite mixed state is called separable if and only if it is possible to express it in the form

$$\rho = \sum_{i=1}^{n} p_i \, |a_i\rangle\langle a_i| \times |b_i\rangle\langle b_i|, \tag{22}$$

where the pure one-particle states $|a_i\rangle$ and $|b_i\rangle$ refer to the first (electron) and second (atom) particle, respectively. The parameters $p_i \geqslant 0$ denote the relevant probabilities. If no transformation of a given density matrix ρ to the form (22) can be given, the system is said to be nonseparable or entangled. Peres [27] and Horodecki *et al.* [28] derived a convenient criterion which, in the case of a 4×4 density matrix, yields a necessary and sufficient condition for separability. For this, we construct the partial transpose density matrix $\rho^{\rm PT}$ where only the variables of one subsystem are transposed:

$$\langle M'm'|\rho^{\rm PT}|Mm\rangle = \langle Mm'|\rho|M'm\rangle. \tag{23}$$

Applying this to the density matrix (16) we obtain

$$\rho^{\rm PT} = \frac{1}{4}\begin{pmatrix} 1+P & 0 & 0 & 2P \\ 0 & 1-P & 0 & 0 \\ 0 & 0 & 1-P & 0 \\ 2P & 0 & 0 & 1+P \end{pmatrix}. \tag{24}$$

A given density matrix ρ describes a separable state if *all* eigenvalues of $\rho^{\rm PT}$ are positive. In contrast, ρ describes an entangled system if at least one eigenvalue is negative [27,28]. Calculating the eigenvalues λ_i of $\rho^{\rm PT}$ yields

$$\lambda_{1,2,3} = \frac{1}{4}(1-P) \quad \text{and} \quad \lambda_4 = \frac{1}{4}(1+3P). \tag{25}$$

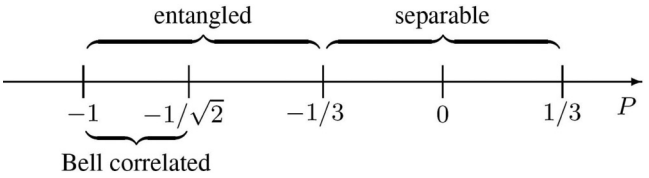

FIG. 1. Separable, entangled, and Bell correlated areas (see text).

Equation (25) indicates that all eigenvalues are positive for P values in the range

$$-\frac{1}{3} \leqslant P \leqslant \frac{1}{3}, \tag{26a}$$

and that the scattering matrix ρ is separable in this region. The density matrix ρ describes an entangled system in the range

$$-1 \leqslant P < -\frac{1}{3}, \tag{26b}$$

where λ_4 becomes negative. The system is maximally entangled for $P = -1$. The results are depicted in Fig. 1.

In conclusion, whether a given collision system is separable or nonseparable depends on the strength of the spin correlation and can be decided experimentally by measuring P.

V. DISCUSSION OF SEPARABILITY

We will now illustrate the abstract results of the preceding section by constructing explicit expressions which will give further insight. Decomposition of mixed states is not unique. However, if it is possible to transform the scattering matrix to the form (22), then ρ is separable. In general, this task is very cumbersome. In our case of interest though, it is rather simple, since the results (14) provide the essential hints. We derive the results for positive and negative values of P separately.

A. Positive correlation parameters

If P is positive, then the spins of the collision pairs are predominantly parallel oriented as follows from (13) and similar equations. The spin system remains separable in this case as shown in Fig. 1. As discussed in Sec. III, the spins of the two collision partners are always correlated, but the correlations are not strong enough for generating entanglement.

Inserting explicitly $P = |P|$, we rewrite the spin density matrix (16) by subtracting a term proportional to the four-dimensional unit matrix. The remaining matrix can then be expressed in terms of the three triplet states $|S = 1 M_s\rangle$ with $M_s = -1, 0, 1$, respectively. We obtain

$$\begin{aligned} \rho &= \frac{1-3|P|}{4}\mathbb{1} + \frac{|P|}{2}\begin{pmatrix} 2 & 0 & 0 & 0 \\ 0 & 1 & 1 & 0 \\ 0 & 1 & 1 & 0 \\ 0 & 0 & 0 & 2 \end{pmatrix} \\ &= \frac{1-3|P|}{4}\mathbb{1} + |P| \sum_{M_s} |1M_s\rangle\langle 1M_s|. \end{aligned} \tag{27}$$

The 4×4 unit matrix $\mathbb{1}$ describes a completely uncorrelated mixture of states, e.g.,

$$\mathbb{1} = \sum_i |a_i b_i\rangle\langle a_i b_i| \quad \text{with} \quad a_i, b_i \in \{\uparrow, \downarrow\}, \tag{28}$$

where the two particles can be found in any of the four separable states with equal probability $\frac{1}{4}$. The four states occurring in (28), and the states $|11\rangle = |\uparrow\uparrow\rangle$ and $|1-1\rangle = |\downarrow\downarrow\rangle$ in (27) are clearly separable, but the Bell state $|10\rangle = \frac{1}{\sqrt{2}}(|\uparrow\downarrow\rangle + |\downarrow\uparrow\rangle)$ is maximally entangled. One might assume that ρ is at least partially entangled, but Fig. 1 shows that ρ is separable for all allowed positive values of P. We will now construct such a representation. Guided by the results (14) for the correlation parameter we start by considering the spin density matrix

$$\begin{aligned}\rho_1 = \tfrac{1}{6}(&|\uparrow_x\rangle\langle\uparrow_x| \times |\uparrow_x\rangle\langle\uparrow_x| + |\downarrow_x\rangle\langle\downarrow_x| \times |\downarrow_x\rangle\langle\downarrow_x| \\ &+ |\uparrow_y\rangle\langle\uparrow_y| \times |\uparrow_y\rangle\langle\uparrow_y| + |\downarrow_y\rangle\langle\downarrow_y| \times |\downarrow_y\rangle\langle\downarrow_y| \\ &+ |\uparrow_z\rangle\langle\uparrow_z| \times |\uparrow_z\rangle\langle\uparrow_z| + |\downarrow_z\rangle\langle\downarrow_z| \times |\downarrow_z\rangle\langle\downarrow_z|),\end{aligned} \tag{29}$$

where $|\uparrow_i\rangle$ and $|\downarrow_i\rangle$ denote particle states with *spin up* ($\uparrow$) and *spin down* ($\downarrow$) with respect to the i axis ($i = x, y, z$). It is

$$|\uparrow_x\rangle = \frac{1}{\sqrt{2}}(|\uparrow\rangle + |\downarrow\rangle), \quad |\uparrow_y\rangle = \frac{1}{\sqrt{2}}(|\uparrow\rangle + \mathrm{i}|\downarrow\rangle),$$

and

$$|\downarrow_x\rangle = \frac{1}{\sqrt{2}}(|\uparrow\rangle - |\downarrow\rangle), \quad |\downarrow_y\rangle = \frac{1}{\sqrt{2}}(|\uparrow\rangle - \mathrm{i}|\downarrow\rangle),$$

while

$$|\uparrow_z\rangle = |\uparrow\rangle \quad \text{and} \quad |\downarrow_z\rangle = |\downarrow\rangle. \tag{30}$$

The state (29) is of the general form (22) and clearly separable. It can be prepared by two spatially separated observers, commonly called Alice and Bob, in an entirely classical way, i.e., by agreeing over the phone on the local preparation of their respective states. For instance, Alice prepares a subset of electrons locally in the state $|\uparrow_x\rangle$. She communicates this to Bob via a classical channel, e.g., phone, see Fig. 2. Then, Bob will prepare the corresponding subset of his particles, hydrogenlike atoms, in the same spin state.

This operation is repeated for the other five states in (29). The beams created by Alice and Bob remain spatially separated without interaction. The total final spin system is then described by the matrix ρ_1 which contains the full information on the system. Any mixed state which is prepared in this way by local operations and classical communication (LOCC) contains correlated spins, but these correlations are created entirely by classical means. By contrast LOCC cannot be used to create entangled states [3]. Calculation of the correlation parameters for ρ_1 by means of (10) yields the results

$$P_i \times P_i = \frac{1}{3} \quad (i, j = x, y, z), \tag{31}$$

and $P_i \times P_j = 0$ for $i \neq j$. The individual polarization vectors vanish. In particular, we get $P_a \times P_a = \frac{1}{3}$, for any direction $\boldsymbol{a}$ of the two spin detector systems. Comparing this with (14), we see that the two spin systems have the same rotational

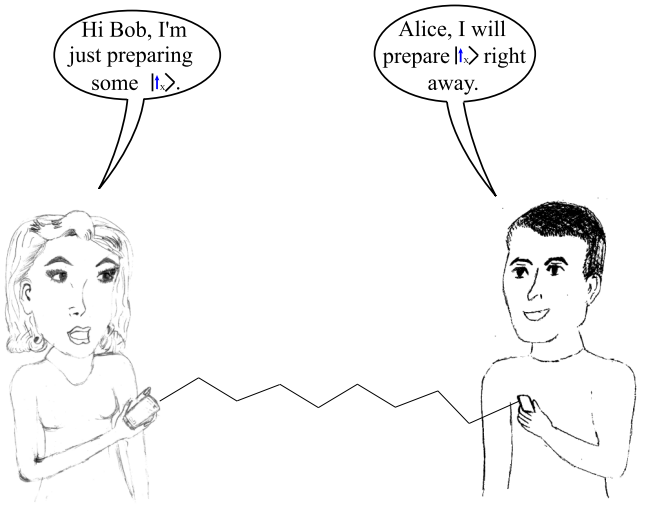

FIG. 2. At her place, Alice prepares a subset of electrons locally in the state $|\uparrow_x\rangle$. She communicates this to Bob via her smart phone, i.e., she is using a classical communication channel. After receiving this message, Bob will prepare the corresponding subset of his particles, hydrogenlike atoms, in the same spin state $|\uparrow_x\rangle$.

symmetry. Only the magnitudes of the correlation parameters differ ($P_i \times P_i = \frac{1}{3}$ in case of ρ_1, and $0 \leqslant P_i \times P_i = P \leqslant \frac{1}{3}$ for ρ). The correlations contained in ρ_1 can be reduced by mixing ρ_1 with a completely uncorrelated system, described by the 4×4 unit matrix (28), until this mixture contains the same amount of correlations as ρ. In order to achieve this we write the spin density matrix (27) as a superposition of the normalized identity matrix $\frac{1}{4}\mathbb{1}$ and ρ_1,

$$\rho = \frac{a}{4}\mathbb{1} + b\,\rho_1, \tag{32}$$

and determine the coefficients a and b by requiring that both sides of (32) must have the same trace, which gives $a + b = 1$, and the same correlation parameters, resulting in $|P| = \frac{1}{3}b$. Thus, we obtain for the spin scattering matrix (27) the expression

$$\rho = \frac{1 - 3|P|}{4}\mathbb{1} + 3|P|\rho_1. \tag{33}$$

Remembering (22) we obtain from (33) that the spin matrix ρ is separable if $|P| \leqslant \frac{1}{3}$ (see Fig. 1) which is in accordance with the Peres-Horodecki criterion.

The essential point is that, on the left-hand side of (33), we have the spin matrix (27) describing the spin correlations between colliding pairs of spin-1/2 particles. On the right-hand side, we have a mixture of $\mathbb{1}$ and ρ_1 which can be prepared by LOCC. Both systems, ρ and the mixture, coincide in all measurable polarization and correlation parameters and are therefore physically indistinguishable. Without prior knowledge it is impossible to decide which system is created in the final state of a scattering experiment, and which system has been prepared by LOCC. This discussion illustrates the meaning of *separability*.

Of course, there are many different ways of preparing the same state ρ. But produced in a collision, the important point is, the spin correlations of separable systems can be reproduced

entirely by a classical mechanism. Hence, it is quite reasonable to state that separable states contain no entanglement.

Finally, comparing (27) and (33), we obtain

$$\rho_1 = \frac{1}{3}\sum_{M_s} |1M_s\rangle\langle 1M_s|. \tag{34}$$

This result is remarkable as the normalized sum over the three triplet states is always separable, though (34) contains the maximally entangled triplet state $|10\rangle = \frac{1}{\sqrt{2}}(|\uparrow\downarrow\rangle + |\downarrow\uparrow\rangle)$.

B. Negative correlations

Now we consider anticorrelated spins. Inserting $P = -|P|$ in (16) we can write the scattering matrix ρ in form of a Werner state [21]

$$\rho = \frac{1-|P|}{4}\mathbb{1} + \frac{|P|}{2}\begin{pmatrix} 0 & 0 & 0 & 0 \\ 0 & 1 & -1 & 0 \\ 0 & -1 & 1 & 0 \\ 0 & 0 & 0 & 0 \end{pmatrix}$$

$$= \frac{1-|P|}{4}\mathbb{1} + |P||00\rangle\langle 00|, \tag{35}$$

where

$$|00\rangle = \frac{1}{\sqrt{2}}(|\uparrow\downarrow\rangle - |\downarrow\uparrow\rangle) \tag{36}$$

is the singlet state. The Werner state (35) represents a mixture of the completely uncorrelated state (28) $\sim \mathbb{1}$ (with amount $1-|P|$) and the maximally entangled singlet state. The magnitude $|P|$ of the correlation parameter plays the role of a mixing parameter in the Werner state. From the Peres-Horodecki criterion, it follows that the state (35) is separable for $0 \geqslant P \geqslant -\frac{1}{3}$ (see Fig. 1). We illustrate this result by explicit construction, following essentially the same procedure as in the preceding case. Since the correlations are negative we consider the density matrix ρ_2 with anticorrelated spins,

$$\begin{aligned}\rho_2 = \tfrac{1}{6}(&|\uparrow_x\rangle\langle\uparrow_x| \times |\downarrow_x\rangle\langle\downarrow_x| + |\downarrow_x\rangle\langle\downarrow_x| \times |\uparrow_x\rangle\langle\uparrow_x| \\ &+ |\uparrow_y\rangle\langle\uparrow_y| \times |\downarrow_y\rangle\langle\downarrow_y| + |\downarrow_y\rangle\langle\downarrow_y| \times |\uparrow_y\rangle\langle\uparrow_y| \\ &+ |\uparrow_z\rangle\langle\uparrow_z| \times |\downarrow_z\rangle\langle\downarrow_z| + |\downarrow_z\rangle\langle\downarrow_z| \times |\uparrow_z\rangle\langle\uparrow_z|).\end{aligned} \tag{37}$$

As ρ_2 is of the form (22) it is separable and hence can be prepared by LOCC. The only nonvanishing components of the correlation tensor are given by

$$P_i \times P_i = -\frac{1}{3} \quad (i = x,y,z). \tag{38}$$

Repeating the steps from (29) to (33) we can rewrite the Werner state (35) in the explicit separable form ($0 \geqslant P \geqslant -\frac{1}{3}$)

$$\rho = \frac{1-3|P|}{4}\mathbb{1} + 3|P|\rho_2. \tag{39}$$

Both sides of (39) are normalized and are characterized by the same set (14) of correlation parameters. They are therefore physically indistinguishable. The discussion following (33) applies directly to (39). The Bloch representation of ρ_2 follows directly from (18) with $P = -\frac{1}{3}$. This value of P divides the separable and entangled parts in Fig. 1. Therefore, ρ_2 can be interpreted as that separable state which is nearest to the entanglement region.

VI. QUANTIFICATION OF ENTANGLEMENT: IMPORTANCE OF NONLOCALITY

We now consider the range $-\frac{1}{3} > P \geqslant -1$ of Fig. 1 where the density matrix (35) represents an entangled spin state according to the Peres-Horodecki condition. The presence of entangled spin pairs can be verified experimentally on the basis of one local coincidence measurement, the determination of P.

The amount of entanglement, produced in the spin system ρ during the collision, can be quantified using the concept of negativity [29,30] which is directly related to the Peres-Horodecki criterion (see Sec. IV). The negativity is defined as

$$N(\rho) = -2\sum_i n_i, \tag{40}$$

where the n_i are the negative eigenvalues of the partial transpose density matrix ρ^{PT}. If all eigenvalues are positive, the corresponding density matrix is separable, and $N(\rho)$ vanishes. Thus, $N(\rho)$ "measures" the amount by which ρ^{PT} fails to be positive definite, and it is intuitively sensible to use $N(\rho)$ as a measure for the entanglement present in the system ρ [30].

In our case of interest, only the eigenvalue λ_4 in (25) can become negative. Hence, for $P < -\frac{1}{3}$, we have

$$N(\rho) = -2\lambda_4 = \frac{1}{2}(3|P| - 1). \tag{41}$$

The negativity is proportional to the magnitude $|P|$ of the correlation parameter and is equal to one for maximal entanglement ($P = -1$), and equals zero for zero entanglement ($P = -\frac{1}{3}$).

These abstract results can be interpreted in the following way. Setting $|P| = \frac{1}{3}$ in (35) and (39) and combining both results we obtain

$$\rho_2 = \frac{2}{3}\left(\frac{1}{4}\mathbb{1}\right) + \frac{1}{3}|00\rangle\langle 00|. \tag{42}$$

Hence, by mixing the maximally entangled singlet state with the (normalized) identity matrix (28) in the ratio 2 : 1 one obtains the separable state ρ_2, which is *nearest* to the entanglement region in Fig. 1. By definition, the mixture on the right-hand side of (42) contains no entanglement, and all correlations contained in this mixture can be classically reproduced. Taking this result into account we write the density matrix (35) in the form

$$\begin{aligned}\rho &= (1-|P|)\left(\frac{1}{4}\mathbb{1} + \frac{1}{2}|00\rangle\langle 00|\right) + \frac{3|P|-1}{2}|00\rangle\langle 00| \\ &= \frac{3}{2}(1-|P|)\rho_2 + \frac{3|P|-1}{2}|00\rangle\langle 00|,\end{aligned} \tag{43}$$

and, using (41), we finally rewrite the Werner state (35) in the form ($-\frac{1}{3} > P \geqslant -1$)

$$\rho = (1-N)\rho_2 + N|00\rangle\langle 00|. \tag{44}$$

Equation (44) shows that the entangled part of the final collision system is determined by the negativity. Thus, $N(\rho)$

measures the amount of entanglement, contained in the system ρ, after all *classical* correlation terms $\sim\rho_2$ have been separated off from the original singlet contribution. Only this fraction is useful for further entanglement studies.

It might be useful for the following discussion to compare the states ρ_2 and $|00\rangle$ in more detail. The singlet state is inherently nonlocal. A spin measurement on one of the particles (say, the free electron) fixes instantaneously the spin state of the second particle (atomic electron) independently of how far the particles are separated from each other. If the first has been found with its spin directed along a specific direction, the second particle will be found with certainty with its spin pointing in the opposite direction.

On the other hand, ρ_2 can be prepared by Alice and Bob in a local way as described in Sec. V B. Each particle is in a well defined spin state, and the correlations have been fixed in advance by Alice and Bob. Furthermore, each particle of a spin pair is not affected by what happens to its partner. That is, ρ_2 behaves in a *local realistic* manner.

Comparing the spin correlations we obtain from (15)

$$P_a^{(1)} \times P_b^{(2)} = -\cos\beta, \tag{45a}$$

for the singlet state, and

$$P_a^{(1)} \times P_b^{(2)} = -\frac{1}{3}\cos\beta, \tag{45b}$$

for ρ_2 where we have applied (38). We remember that $|P| = \frac{1}{3}$ is the largest value of the correlation parameter which can be obtained by LOCC methods. Hence, the inherent nonlocality of the singlet state produces correlations three times as strong as the best result that can be achieved by classical local methods.

It is remarkable that the two systems, which are as fundamentally different as $|00\rangle$ and ρ_2, can be combined in an expression as simple as (44). Similar relations can be derived for other Bell states.

Eventually we compare the mixed states briefly with pure spin states. In collisions between two spin-1/2 beams, which are initially completely polarized, the final combined spin state is necessarily a pure state. In this case the amount of entanglement is quantified by the magnitudes $|\boldsymbol{P}^{(1)}| = |\boldsymbol{P}^{(2)}|$ of the two individually measured polarization vectors (see, e.g., Sec. 3.6.5 of [22]). The final spin system is maximally entangled if the polarization vectors vanish. These results are contained in the negativity as a special case.

VII. BELL CORRELATIONS

Entanglement is inherently a nonlocal phenomenon. In order to avoid this *strange* feature of quantum mechanics some researchers introduced hypothetical *hidden variables* [4,5] hoping to reinstate the results of conventional quantum mechanics in a Newtonian local realistic way. Although designed to preserve locality it has turned out that they were unable to do so in all circumstances. As a consequence of Bell's theorem [5] a set of inequalities have been derived, collectively known as Bell inequalities, which must be satisfied by any local theory, and which can be used as a test of its validity.

A quantum mechanical state is said to display nonlocal correlations, or being Bell (or EPR) correlated, if it violates any of the Bell inequalities. Whereas pure entangled spin-1/2 states are necessarily Bell correlated [31–34], this is in general not the case for mixed entangled states. This surprising result, which is of fundamental importance for the foundations of quantum mechanics, was first demonstrated by Werner [21] who proved that a state of the form (35) is only Bell correlated if the condition $P < -\frac{1}{\sqrt{2}}$ is satisfied; from (41), we get $N(\rho) \geqslant 0.56$ for the negativity in this case.

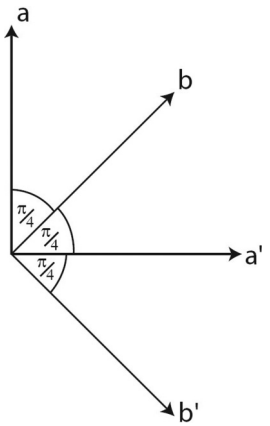

FIG. 3. Coplanar directions of the detector-spin-analyzer sets (see text).

Following Aspect *et al.* [35], we will adapt this to our case of interest. Consider the following combination of correlation parameters:

$$\Delta(\boldsymbol{a},\boldsymbol{a}',\boldsymbol{b},\boldsymbol{b}') = \left|P_a^{(1)} \times P_b^{(2)} - P_a^{(1)} \times P_{b'}^{(2)}\right| + \left|P_{a'}^{(1)} \times P_b^{(2)} + P_{a'}^{(1)} \times P_{b'}^{(2)}\right|, \tag{46}$$

where $\boldsymbol{a},\boldsymbol{a}',\boldsymbol{b}$,and $\boldsymbol{b}'$ denote four unit vectors referring to the directions of the detector-spin-analyzer sets in the corresponding coincidence measurement of the first (directions $\boldsymbol{a}$ and $\boldsymbol{a}'$) and second beam (directions $\boldsymbol{b}$ and $\boldsymbol{b}'$), respectively. Based on Bell's work [5], it has been shown by Clauser *et al.* [6] that local realism implies the familiar CHSH inequality

$$\Delta(\boldsymbol{a},\boldsymbol{a}',\boldsymbol{b},\boldsymbol{b}') \leqslant 2, \tag{47}$$

which has been more generally derived by Bell himself, shortly after [36]. Quantum mechanics allows a larger bound, known as Cirel'sons bound [37]

$$\Delta(\boldsymbol{a},\boldsymbol{a}',\boldsymbol{b},\boldsymbol{b}') \leqslant 2\sqrt{2}. \tag{48}$$

In order to demonstrate that local hidden variable theories are inconsistent with quantum mechanics it is only necessary to show that condition (47) is violated for a particular setting of the measurement apparatus.

Considering coplanar vectors, as shown in Fig. 3, the angles between the different directions are not independent. Assuming the angles between $\boldsymbol{a}$ and $\boldsymbol{b}$,$\boldsymbol{b}$ and $\boldsymbol{a}'$, and $\boldsymbol{a}'$ and $\boldsymbol{b}'$ equal to $\frac{\pi}{4}$, the remaining angle between $\boldsymbol{a}$ and $\boldsymbol{b}'$ is equal to $\frac{3\pi}{4}$.

Calculating the correlation parameters using (15) one obtains from (46)

$$\Delta = 2\sqrt{2}\,|P|. \tag{49}$$

It follows that the inequality (47) is violated for all correlation parameters with $P < -1/\sqrt{2}$. Thus, as depicted in Fig. 1, the spin system (35) is entangled in the range $-\frac{1}{3} > P > -\frac{1}{\sqrt{2}}$ but does not violate any Bell inequalities since the spin correlation in this region is not sufficiently strong and it is in principle possible to simulate the quantum correlations within local theories. This possibility is ruled out for values $-1 \leqslant P < -\frac{1}{\sqrt{2}}$ by Bell's theorem. In this case, the correlations, generated by the spin-exchange collision, are stronger than could ever be created by classical means and cannot be described by local realistic theories. For $P = -1$, (49) yields a maximal violation of the CHSH inequality (47), or any other of the Bell inequalities.

VIII. DISCUSSION OF EXPERIMENTAL AND NUMERICAL RESULTS

As the crucial question, we discuss how strong the spin correlations are which can be produced during the elastic collision process out of an initial totally chaotic spin system, and without the influence of explicit spin-dependent interaction. In order to get some insight into the relationship between scattering dynamics and entanglement properties, we analyze published experimental and numerical data for the spin asymmetry $A_{\rm ex}$ which, applying (21), we reinterpret in terms of the spin correlation parameter P.

First in the field, investigating spin-dependent elastic e-H scattering were Burke and Schey [38]. They derived general equations for the various possible observables for arbitrary initial conditions of the two spin systems, and published numerical results for collision energies around and below 10 eV, while employing a rather crude approach from a nowadays view. Combining two of their observables, results for the entanglement parameter P can be obtained, though, it turns out that the final spin state remains practically separable, except for the lowest energy at $E = 1.36$ eV. Later on, several groups investigated spin-dependent elastic e-H scattering, e.g., see [39–43]. However, in the energy region studied (0.14 to 300 eV), the data corroborate the results of Burke and Schey indicating that practically no entanglement can be created, except at the lowest energies [42], e.g., see the multipseudostate close coupling (MPCC) data in Fig. 4 at $E = 0.14$, 0.54, and 1.22 eV.

The Bell correlated region can almost not be reached.

Remarkable measurements have been performed on spin-dependent elastic e-Na scattering by the NIST group [26,44–47]. We have selected experimental data at 4.1, 10, and 20 eV (see Fig. 5), and at 1.6 and 12.1 eV (see Fig. 6), demonstrating that the correlation parameter P may vary over the full region from $P = \frac{1}{3}$ (fully separable) down to $P = -1$ (fully entangled) and thus, any degree of entanglement or even Bell correlation can be reached.

For example, for $E = 4.1$ eV, the data reveal pronounced entanglement effects between about 80° and 105° with a sharp minimum around $\theta = 90°$), with $P \simeq -0.87$ and negativity $N(\rho) \simeq 0.81$. These data are well in the Bell correlated area.

Even more striking are the results for $E = 10$ eV, where P decreases rapidly around $\theta = 60°$ to values near $P = -1$. Here the spins of the colliding pairs form intermediately the maximally entangled singlet state, and the Werner state (44)

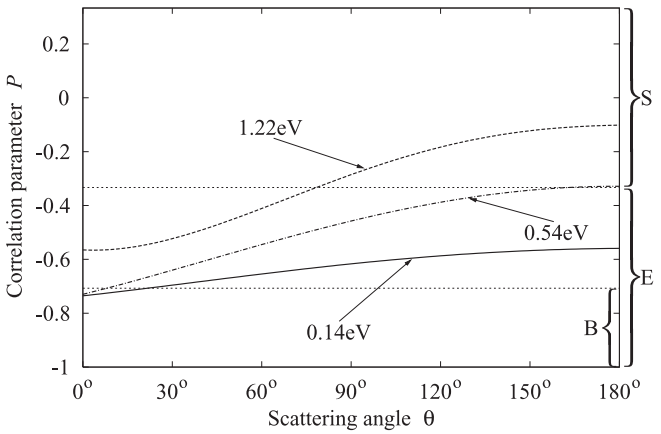

FIG. 4. Correlation parameter P of hydrogen versus scattering angle θ for different scattering energies. Numerical data: 0.14, 0.54, and 1.22 eV, (MPCC) van Wyngaarden and Walters [42]. Horizontal lines divide separable (S), entangled (E), and Bell correlated (B) regions.

is dominated by the singlet contribution with negativity $N(\rho) = 1$. A similar behavior is shown for the experimental data at $E = 12.1$ eV (see Fig. 6), where P reveals a sharp minimum with negativity $N(\rho) \simeq 1$ near $\theta = 53°$. These data are in excellent agreement with convergence close coupling (CCC) [48–50] and coupled channel optical (CCO) calculations [51], respectively, as shown in Figs. 5 and 6. For energies around the $3p$ threshold (2.1 eV) or higher, close coupling (CC) data are available [52] elucidating considerable degrees of entanglement up to $N(\rho) \simeq 1$. For example, for $E = 2.2$ eV and $E = 2.05$ eV, we obtain $P \simeq -1$ at $\theta \simeq 107.5°$ and $\theta \simeq 105°$, respectively (see Figs. 5 and 6). Even for 5.0 eV the CC data exhibit a minimum of $P \simeq -0.93$ around $\theta = 85°$ as shown in Fig. 6, elucidating that the Bell correlated area is attainable over a broad region of energy. On the other hand, the NIST data reveal that for $E = 1.0$ and 1.6 eV,

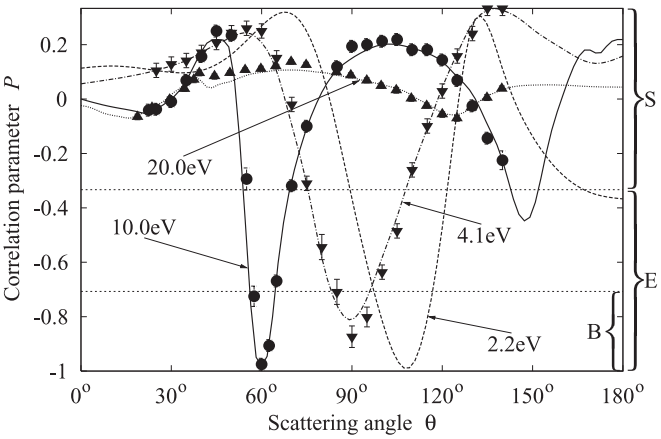

FIG. 5. Correlation parameter P of sodium versus scattering angle θ for different scattering energies. Experimental data by NIST group: 4.1 eV (▼), McClelland *et al.* [44,47]; 10 eV (●) and 20 eV (▲), Kelley *et al.* [46]. Numerical data: 2.2 eV, (CC) Moores and Norcross [52]; 4.1, 10, and 20 eV (CCC) Bray [48,49]. Horizontal lines divide separable (S), entangled (E), and Bell correlated (B) regions.

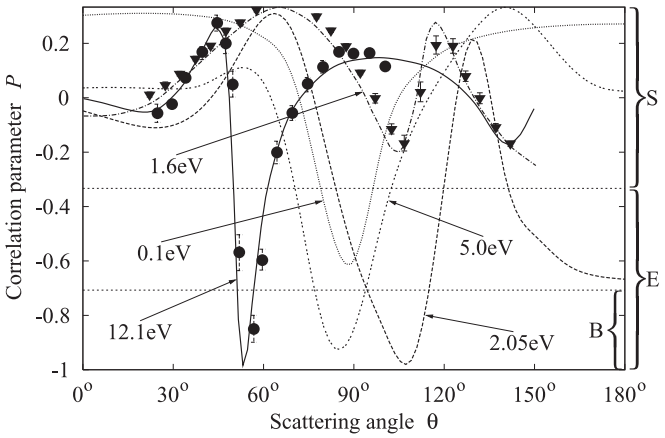

FIG. 6. Correlation parameter P of sodium versus scattering angle θ for different scattering energies. Experimental data by NIST group: 1.6 eV (▼), Lorentz *et al.* [26]; 12.1 eV (•), McClelland *et al.* [47]. Numerical data: 0.1, 2.05, and 5.0 eV (CC) Moores and Norcross [52]; 1.6 eV, (CCC) Bray [49]; 12.1 eV, (CCO) Bray and McCarthy [51]. Horizontal lines divide separable (S), entangled (E), and Bell correlated (B) regions.

the latter shown in Fig. 6, as well as for $E = 20$ eV (see Fig. 5) and larger energies, practically no entanglement can be produced. However, for small energies $E = 0.1$ eV (see Fig. 6) the CC data again enter the entanglement area with a minimum of $P \simeq -0.61$ at $\theta = 88°$, indicating the strong energy dependence of the spin-spin correlations. The Bell correlated area cannot be reached in this energy region.

Interestingly, similar behavior is observed in experimental data on elastic e-Li scattering [53]. The Li data are in generally good agreement with CCO calculations [54]. Here the asymmetry was measured as a function of the collision energy at fixed scattering angles as depicted in Fig. 7 which, moreover, provides good examples for the different cases of separable, entangled, and Bell correlated states.

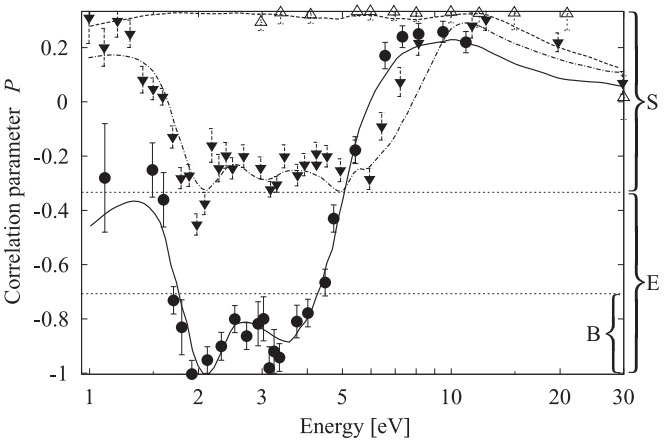

FIG. 7. Correlation parameter P of Li versus electron projectile energy in the range $E = 1$–30 eV for fixed scattering angles $\theta = 65°(\triangle), 90°(\blacktriangledown), 107.5°(\bullet)$. Experimental data: Baum *et al.* [53]. Numerical data: 13CCO8 calculation, Bray *et al.* [54]. Horizontal lines divide separable (S), entangled (E), and Bell correlated (B) regions.

For a scattering angle of $\theta = 65°$ and up to $E \sim 20$ eV the correlation parameter is nearly constant with value $P \simeq \frac{1}{3}$. The final state in this region, given by the separable density matrix ρ_1, is practically independent of the scattering energy. ρ_1 can be written as a sum over the three triplet states (34) or in the explicit separable form (29). Alternatively, one can think of the final spins of the combined e-Li system as paired up exactly parallel oriented, and the spin pairs are equally distributed over all spatial directions (see Sec. V A). For $\theta = 90°$, the combined spin system is separable for all energies except a small region around $2p$ threshold at 1.84 eV, where the experimental data already indicate an entanglement of $P \sim -0.45$. For energies between about $E \simeq 2$ and 6 eV, the lower bound of the separable region $P \simeq -\frac{1}{3}$ is reached, and the final state can be approximately represented by the density matrix ρ_2 which may be expressed either by (42) or, alternatively, by the explicit separable expression (37). Because of its rotational invariance the final spin system can be considered as consisting of pairs with antiparallel spins, equally distributed over all spatial directions (see Sec. V B). In contrast, for $\theta = 107.5°$, see Fig. 7, the correlation parameter decreases rapidly to $P = -1$ around $2p$ threshold and remains low up to $E \simeq 4$ eV. In this energy region, the anticorrelations are strong enough to generate entanglement with negativity $N(\rho) \simeq 1$. In this case, we read off from (44) that the Werner state is almost solely represented by the inherently nonlocal singlet state (see Sec. VI).

Let us consider the experimental and numerical sodium results of Figs. 5 and 6, and the lithium data of Fig. 7 in more detail. The two most remarkable points to note are the following. First, the results show that correlations with $P \simeq -1$ can be obtained. Then, the spins of the final collision partners are practically completely anticorrelated and form very nearly a singlet state, independently of how far they are separated again after the collision. These states violate the CHSH inequality (47) almost maximally, providing strong evidence for the existence of nonlocal effects. Second, it is remarkable that in several cases the correlation parameter varies nearly over the full allowed range $[-1, \frac{1}{3}]$ for both, as a function of θ, and as a function of E. This allows for interesting practical applications where Figs. 5–7 can be used as a guide. One can prepare a spin-spin correlated system by scattering unpolarized electrons from unpolarized atoms (Na, Li), choosing particular values for scattering angle, and/or energy, and can read off from Figs. 5–7 the value of the corresponding spin correlation parameter without need of a further measurement. In this way any desired degree of entanglement, and corresponding negativity $N(\rho)$, between the collision spin pairs can be prepared. In particular, the singlet state can readily be generated by tuning to the appropriate experimental parameters. These systems are then available for further experiments, where a source of strongly correlated particle pairs is required, capable of transmitting nonlocal information; for example in quantum teleportation or quantum cryptography studies.

This possibility might be of practical importance. For example, while it has been shown [55], that any mixed system of two spin-$\frac{1}{2}$ states which violates the Bell-CHSH inequality (47) is useful for teleportation [14], Popescu[56] provided arguments that states, which do not violate Bell's

inequalities, could still be used for teleportation, and stressed the need for an experimental verification. We refer to the review by Brunner *et al.* [1] for further details. For such an experiment one would need collision pairs with values $-\frac{1}{3} \geqslant P \geqslant -\frac{1}{\sqrt{2}}$ for the correlation parameter. Such states could be prepared, for example, by scattering electrons from sodium atoms at $E = 10.0$ or 12.1 eV and choosing a scattering angle as indicated by Fig. 5 or 6. Alternatively, electrons could be scattered from lithium atoms at $\theta = 107.5°$, choosing the appropriate scattering energy from Fig. 7.

However, it should be remembered that for states, less entangled then the singlet state, only a fraction of the final collision pairs can be used for subsequent entanglement-dependent studies. From (41) we find $N(\rho)$ varying between zero for $P = -\frac{1}{3}$ and $N(\rho) = 0.561$ for $P = -\frac{1}{\sqrt{2}}$ in this case.

All together, the results in Figs. 4–7 may provide a practical tool for new testing grounds of nonlocal effects. In this context the physics of scattering meets quantum information and quantum computation.

IX. CONCLUSIONS

In the present paper we have discussed under which conditions entanglement can be generated in elastic collisions between electrons and light, pseudo (or truly) one-electron atoms, both initially unpolarized. Both beams have been prepared independently from each other and had never been in contact before the collision. Explicit spin-dependent forces have been neglected which is a good approximation for light atoms.

We have shown that the full information on the entanglement properties of the final mixed spin system is contained in one single parameter, the spin correlation parameter P, which is a function of scattering angle and energy. The areas of P, where the spins of the collision partners remain separable, or are entangled, or even Bell correlated, have been identified. Experimentally, the presence of entangled spin pairs can be verified on the basis of one local measurement via the determination of P. The amount of entanglement, produced during the collision, is given by the negativity $N(\rho)$.

Analyzing published numerical and experimental data on the spin asymmetry A_{ex}, we have obtained results for the spin correlation parameter P. Figures 4–7 reveal the unexpected result that surprisingly strong spin correlations can be created out of an initially totally chaotic spin system. In particular, Bell correlated spin pairs have been obtained, violating the CHSH equation even maximally, with $P \simeq -1$. This is proof that the electron exchange process under discussion is intrinsically nonlocal.

Considering the remarkable experiments, presented in [8–10], we emphasize that our results originate from a completely unrelated field of research and refer to experiments with massive particles. The results yield therefore additional support to the thesis that nature behaves quantum mechanically and nonlocally.

By performing the described scattering experiment Bell pairs can be produced quickly and repeatable in the full range between $P = -\frac{1}{\sqrt{2}}$ and $P = -1$. By studying the data in Figs. 4–7 one can tune to a particular scattering angle and energy, and create pairs of collision partners with any desired degree of spin entanglement. In particular, the singlet state can readily be generated in the collision. These pairs can then be used for further experiments where pairs of particles with a high degree of correlation are required. This might be of interest for quantum communication or teleportation studies and might lead to a certain *entanglement* between scattering physics and quantum information.

ACKNOWLEDGMENTS

The authors are thankful to Tanya Lohmann for preparing Fig. 2. B.La. acknowledges financial support by the Bundesministerium für Bildung und Forschung (BMBF) (Contract No. 05K13KE2) within the network FSP-302.

APPENDIX: THE *e*-H COINCIDENCE EXPERIMENT

We stressed the point that our main intention is to provide and describe an entanglement source for subsequent experiments and applications in the field of quantum information and quantum computation. On the other hand, the derived theory of the scattering process allows for a direct measurement of the spin correlations of the collision particles within a spin-spin coincidence experiment. A possible experimental setup is illustrated in Fig. 8.

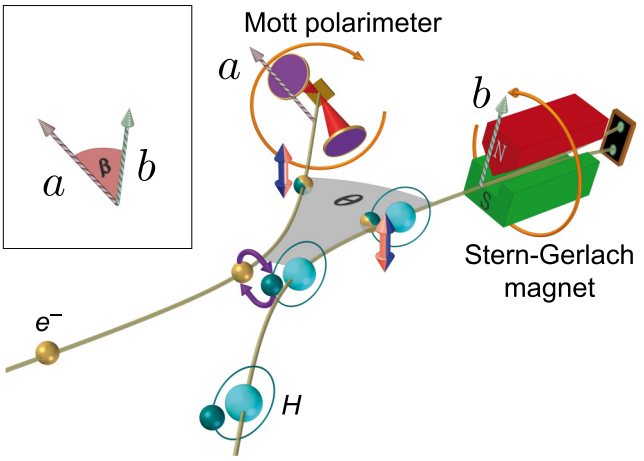

FIG. 8. Scheme of an *e*-H spin correlation coincidence experiment expressed by (A2). The incoming unpolarized electron (gold) is elastically scattered under the angle θ in the Coulombic field of the unpolarized hydrogen atom (blue), where electron exchange with the bound electron (green) can come into effect (purple arrows). This allows for the generation of spin entanglement (red and blue up-down arrows) between the collision partners which is then observed in coincidence by two spin detectors. A Mott polarimeter, oriented with its analyzing axis into direction $\boldsymbol{a}$, analyzes the spin of the scattered electron, while a Stern-Gerlach magnet, oriented with its spin selection axis into direction $\boldsymbol{b}$, is analyzing the spin of the bound electron. The angle β denotes the angle between the orientations $\boldsymbol{a}$ and $\boldsymbol{b}$ of the two spin detectors, shown in the inset. In case of maximal negativity $N(\rho) = 1$, that is for a pure singlet state $|00\rangle$, and for parallel orientations of the two detectors, the Mott polarimeter counts spin-up while the Stern-Gerlach magnet counts spin-down and vice versa.

As discussed in Sec. III, the individual components (9) of the spin polarization vectors of the two subsystems cancel, and the only nonvanishing components of the spin correlation tensor, as given in (14), are expressed by the spin correlation parameter

$$P = P_i^{(1)} \times P_i^{(2)}, \quad i = x,y,z, \tag{A1}$$

where $P = P(\theta,E)$ is a function of scattering angle and energy.

Denoting $\sigma_a = \boldsymbol{\sigma} \cdot \boldsymbol{a}$ as the component of the Pauli operator $\boldsymbol{\sigma}$ in the direction of the unit vector $\boldsymbol{a}$, and $\sigma_b = \boldsymbol{\sigma} \cdot \boldsymbol{b}$ as the component into direction $\boldsymbol{b}$, we are able to generalize (A1) applying the tensorial properties of $P_i^{(1)} \times P_i^{(2)}$.

For instance, if the spin of the first particle, say electron, is measured along direction $\boldsymbol{a}$ via Mott polarimeter techniques, and the spin of the second particle, hydrogenlike atom, along $\boldsymbol{b}$ by means of a Stern-Gerlach magnet (see Fig. 8), the resulting spin correlations are given by the expression

$$P_a^{(1)} \times P_b^{(2)} = P \cos\beta, \tag{A2}$$

where β is the angle between $\boldsymbol{a}$ and $\boldsymbol{b}$ (see inset Fig. 8), which, together with (14), exhibits the rotational symmetry of the spin-spin system. Equation (A2) yields a measurable quantity which can be obtained from a spin-spin correlation coincidence experiment, as depicted in Fig. 8, illustrated for the case of an elastic e-H collision.

In principle, in such spin-spin correlation experiment, and from a theoretical point of view, both directions of the analyzing axes $\boldsymbol{a}$ and $\boldsymbol{b}$ of the two spin detectors can be freely rotated about 4π and may point in any direction for a specific measurement. However, due to the technical analyzing requirements of the Mott polarimeter and the Stern-Gerlach magnet, both vectors, $\boldsymbol{a}$ and $\boldsymbol{b}$, must be oriented perpendicular to the corresponding beam axes of the elastically scattered particles. Nevertheless, both may still be rotated about 2π around their beam axes, as illustrated in Fig. 8. Furthermore, note that the red and blue spin up-down arrows in Fig. 8 only illustrate a certain time sketch of the totally chaotic, spin orientations of the scattered particles. Generally, each single spin of either particle is fully arbitrarily oriented, which is illustrated by the fact that the two individual spin polarization vectors vanish. Though, if both spins are measured in coincidence, they exhibit spin-spin correlations quantified by the spin correlation parameter P.

[1] N. Brunner, D. Cavalcanti, S. Pironio, V. Scarani, and S. Wehner, Bell nonlocality, Rev. Mod. Phys. **86**, 419 (2014).

[2] O. Gühne and G. Tóth, Entanglement detection, Phys. Rep. **474**, 1 (2009).

[3] R. Horodecki, P. Horodecki, M. Horodecki, and K. Horodecki, Quantum entanglement, Rev. Mod. Phys. **81**, 865 (2009).

[4] A. Einstein, B. Podolsky, and N. Rosen, Can quantum-mechanical description of physical reality be considered complete? Phys. Rev. **47**, 777 (1935).

[5] J. S. Bell, On the Einstein-Podolsky-Rosen paradox, Physics **1**, 195 (1964).

[6] J. F. Clauser, M. A. Horne, A. Shimony, and R. A. Holt, Proposed Experiment to Test Local Hidden-Variable Theories, Phys. Rev. Lett. **23**, 880 (1969).

[7] M. D. Reid, P. D. Drummond, W. P. Bowen, E. G. Cavalcanti, P. K. Lam, H. A. Bachor, U. L. Andersen, and G. Leuchs, Colloquium: The Einstein-Podolsky-Rosen paradox: From concepts to applications, Rev. Mod. Phys. **81**, 1727 (2009).

[8] B. Hensen, H. Bernien, A. E. Dréau, A. Reiserer, N. Kalb, M. S. Blok, J. Ruitenberg, R. F. L. Vermeulen, R. N. Schouten, C. Abellán, W. Amaya, V. Pruneri, M. W. Mitchell, M. Markham, D. J. Twitchen, D. Elkouss, S. Wehner, T. H. Taminiau, and R. Hanson, Loophole-free Bell inequality violation using electron spins separated by 1.3 kilometres, Nature (London) **526**, 682 (2015).

[9] M. Giustina, M. A. M. Versteegh, S. Wengerowsky, J. Handsteiner, A. Hochrainer, K. Phelan, F. Steinlechner, J. Kofler, J.-Å. Larsson, C. Abellán, W. Amaya, V. Pruneri, M. W. Mitchell, J. Beyer, T. Gerrits, A. E. Lita, L. K. Shalm, S. W. Nam, T. Scheidl, R. Ursin, B. Wittmann, and A. Zeilinger, Significant-Loophole-Free Test of Bell's Theorem with Entangled Photons, Phys. Rev. Lett. **115**, 250401 (2015).

[10] L. K. Shalm, E. Meyer-Scott, B. G. Christensen, P. Bierhorst, M. A. Wayne, M. J. Stevens, T. Gerrits, S. Glancy, D. R. Hamel, M. S. Allman, K. J. Coakley, S. D. Dyer, C. Hodge, A. E. Lita, V. B. Verma, C. Lambrocco, E. Tortorici, A. L. Migdall, Y. Zhang, D. R. Kumor, W. H. Farr, F. Marsili, M. D. Shaw, J. A. Stern, C. Abellán, W. Amaya, V. Pruneri, T. Jennewein, M. W. Mitchell, P. G. Kwiat, J. C. Bienfang, R. P. Mirin, E. Knill, and S. W. Nam, Strong Loophole-Free Test of Local Realism, Phys. Rev. Lett. **115**, 250402 (2015).

[11] E. Schrödinger, Die gegenwärtige Situation in der Quantenmechanik, Naturwissenschaften **23**, 807 (1935); English translation, The present situation in quantum mechanics, Proc. Am. Philos. Soc. **124**, 323 (1980); reprinted in J. A. Wheeler and M. H. Zurek (eds.) *Quantum Theory and Measurement* (Princeton University Press, Princeton, 1983), p. 152.

[12] N. Herbert, Cryptographic approach to hidden variables, Am. J. Phys. **43**, 315 (1975).

[13] A. Ekert, Quantum Cryptography Based on Bell's Theorem, Phys. Rev. Lett. **67**, 661 (1991).

[14] C. H. Bennett, G. Brassard, Popescu, C. Crépeau, R. Josza, A. Peres, and W. K. Wootters, Teleporting an Unknown Quantum State via Dual Classical and Einstein-Podolsky-Rosen Channels, Phys. Rev. Lett. **70**, 1895 (1993).

[15] D. Gottesman and I. Chuang, Demonstrating the viability of universal quantum computation using teleportation and single-qubit operations, Nature (London) **402**, 390 (1999).

[16] R. Raussendorf and H. J. Briegel, A One-Way Quantum Computer, Phys. Rev. Lett. **86**, 5188 (2001).

[17] K. Blum and B. Lohmann, Entanglement and Bell Correlation in Electron-Exchange Collisions, Phys. Rev. Lett. **116**, 033201 (2016).

[18] N. Andersen and K. Bartschat, *Polarization, Alignment, and Orientation in Atomic Collisions* (Springer, Heidelberg, 2001).

[19] H. Kleinpoppen, B. Lohmann, and A. N. Grum-Grzhimailo, *Perfect/Complete Scattering Experiments—Probing Quantum*

Mechanics on Atomic and Molecular Collisions and Coincidences (Springer, Berlin, 2013).

[20] N. Chandra and R. Ghosh, *Quantum Entanglement in Electron Optics* (Springer, Berlin, 2013).

[21] R. F. Werner, Quantum states with Einstein-Podolsky-Rosen correlations admitting a hidden-variable model, Phys. Rev. A **40**, 4277 (1989).

[22] K. Blum, *Density Matrix Theory and Applications*, 3rd ed. (Springer, Berlin, 2012), in particular Sec. 3.6.5.

[23] J. Kessler, *Polarized Electrons*, 2nd ed. (Springer, Berlin, 1985).

[24] T. Yu and J. H. Eberly, Sudden death of entanglement, Science **323**, 598 (2009).

[25] The description of the spin-spin system in terms of an X matrix is not unusual [24]. It arises naturally in a wide variety of physical situations including pure Bell and mixed Werner states, respectively; see also T. Yu, and J. H. Eberly, Evolution from entanglement to decoherence of bipartite mixed "X" states, Quant. Inf. Comput. **7**, 459 (2007).

[26] S. R. Lorentz, R. E. Scholten, J. J. McClelland, M. H. Kelley, and R. J. Celotta, Spin-Resolved Elastic Scattering of Electrons from Sodium Below the Inelastic Threshold, Phys. Rev. Lett. **67**, 3761 (1991).

[27] A. Peres, Separability Criterion for Density Matrices, Phys. Rev. Lett. **77**, 1413 (1996).

[28] M. Horodecki, P. Horodecki, and R. Horodecki, Separability of mixed states: Necessary and sufficient conditions, Phys. Lett. A **223**, 1 (1996).

[29] K. Zyczkowski, P. Horodecki, A. Sanpera, and M. Lewenstein, Volume of the set of separable states, Phys. Rev. A **58**, 883 (1998).

[30] G. Vidal and R. F. Werner, Computable measure of entanglement, Phys. Rev. A **65**, 032314 (2002).

[31] V. Capasso, D. Fortunato, and F. Selleri, Sensitive observables of quantum mechanics, Int. J. Theor. Phys. **7**, 319 (1973).

[32] N. Gisin, Bell's inequality holds for all non-product states, Phys. Lett. A **154**, 201 (1991).

[33] N. Gisin and A. Peres, Maximal violation of Bell's inequality for arbitrary large spin, Phys. Lett. A **162**, 15 (1992).

[34] S. Popescu and D. Rohrlich, Generic quantum nonlocality, Phys. Lett. A **166**, 293 (1992).

[35] A. Aspect, J. Dalibard, and G. Roger, Experimental Test of Bell's Inequalities Using Time-Varying Analyzers, Phys. Rev. Lett. **49**, 1804 (1982).

[36] J. S. Bell, Introduction to the hidden variable question, in *Foundations of Quantum Mechanics, Proceedings of the International School of Physics Enrico Fermi*, Vol. 171 (Academic, New York, 1971).

[37] B. S. Cirel'son, Quantum generalizations of Bell's inequality, Lett. Math. Phys. **4**, 93 (1980).

[38] P. G. Burke and H. Schey, Polarization and correlation of electron spin in low-energy elastic electron-hydrogen collisions, Phys. Rev. **126**, 163 (1962).

[39] G. D. Fletcher, M. J. Alguard, T. J. Gay, V. W. Hughes, C. W. Tu, R. F. Wainwright, M. S. Lubell, W. Raith, and F. C. Tang, Measurement of Spin-Exchange Effects in Electron-Hydrogen Collisions: 90° Elastic Scattering from 4 to 30 eV, Phys. Rev. Lett. **48**, 1671 (1982).

[40] G. D. Fletcher, M. J. Alguard, T. J. Gay, V. W. Hughes, R. F. Wainwright, M. S. Lubell, and W. Raith, Experimental study of spin-exchange effects in elastic and ionizing collisions of polarized electrons with polarized hydrogen atoms, Phys. Rev. A **31**, 2854 (1985), and references therein.

[41] D. H. Oza and J. Callaway, Spin asymmetry in elastic scattering of electrons by hydrogen atoms, Phys. Rev. A **32**, 2534(R) (1985).

[42] W. L. van Wyngaarden and H. R. J. Walters, Spin asymmetry parameters for electron-hydrogen scattering: I. Elastic scattering, J. Phys. B: At. Mol. Phys. **19**, 1817 (1986). This paper was incorrectly cited in our previous work [17].

[43] I. E. McCarthy and B. Shang, Spin asymmetry in resonant electron-hydrogen elastic scattering, Phys. Rev. A **48**, 1699 (1993).

[44] J. J. McClelland, M. H. Kelley, and R. J. Celotta, Superelastic scattering of spin-polarized electrons from sodium, Phys. Rev. A **40**, 2321 (1989).

[45] R. E. Scholten, S. R. Lorentz, J. J. McClelland, M. H. Kelley, and R. J. Celotta, Spin-resolved superelastic scattering from sodium at 10 and 40 eV, J. Phys. B: At. Mol. Phys. **24**, L653 (1991).

[46] M. H. Kelley, J. J. McClelland, S. R. Lorentz, R. E. Scholten, and R. J. Celotta, in *Correlations and Polarization in Electronic and Atomic Collisions and (e, 2e) Reactions*, edited by P. J. O. Teubner and E. Weigold (Institute of Physics and Physics Society, London, 1992), p. 23.

[47] J. J. McClelland, S. R. Lorentz, R. E. Scholten, M. H. Kelley, and R. J. Celotta, Determination of complex scattering amplitudes in low-energy elastic electron-sodium scattering, Phys. Rev. A **46**, 6079 (1992).

[48] I. Bray, Convergent close-coupling calculation of electron-sodium scattering, Phys. Rev. A **49**, R1 (1994).

[49] I. Bray, Convergent close-coupling method for the calculation of electron scattering on hydrogen like targets, Phys. Rev. A **49**, 1066 (1994).

[50] K. Bartschat and I. Bray, Local versus non-local core potentials in electron scattering from sodium atoms, J. Phys. B: At. Mol. Opt. Phys. **29**, L271 (1996).

[51] I. Bray and I. E. McCarthy, Spin-dependent observables in electron-sodium scattering calculated using the coupled-channel optical method, Phys. Rev. A **47**, 317 (1993).

[52] D. L. Moores and D. W. Norcross, The scattering of electrons by sodium atoms, J. Phys. B: At. Mol. Phys. **5**, 1482 (1972).

[53] G. Baum, M. Moede, W. Raith, and U. Sillmen, Measurement of Spin Dependence in Low-Energy Elastic Scattering of Electrons from Lithium Atoms, Phys. Rev. Lett. **57**, 1855 (1986).

[54] I. Bray, D. V. Fursa, and I. E. McCarthy, Calculation of electron-lithium scattering using the coupled-channel optical method, Phys. Rev. A **47**, 1101 (1993).

[55] R. Horodecki, M. Horodecki, and P. Horodecki, Teleportation, Bell's inequalities and inseparability, Phys. Lett. A **222**, 21 (1996).

[56] S. Popescu, Bell's Inequalities versus Teleportation: What is Nonlocality?, Phys. Rev. Lett. **72**, 797 (1994).